Research Article

Cancer Prevention Research

Lycopene Metabolite, Apo-10′-Lycopenoic Acid, Inhibits Diethylnitrosamine-Initiated, High Fat Diet–Promoted Hepatic Inflammation and Tumorigenesis in Mice

Blanche C. Ip[1,4], Kang-Quan Hu[1], Chun Liu[1], Donald E. Smith[2], Martin S. Obin[3,4], Lynne M. Ausman[1,4], and Xiang-Dong Wang[1,4]

Abstract

Obesity is associated with increased risk in hepatocellular carcinoma (HCC) development and mortality. An important disease control strategy is the prevention of obesity-related hepatic inflammation and tumorigenesis by dietary means. Here, we report that apo-10′-lycopenoic acid (APO10LA), a cleavage metabolite of lycopene at its 9′,10′-double bond by carotene-9′,10′-oxygenase, functions as an effective chemopreventative agent against hepatic tumorigenesis and inflammation. APO10LA treatment on human liver THLE-2 and HuH7 cells dose dependently inhibited cell growth and upregulated sirtuin 1 (SIRT1), a NAD^+-dependent protein deacetylase that may suppress hepatic carcinogenesis. This observed SIRT1 induction was associated with decreased cyclin D1 protein, increased cyclin-dependent kinase inhibitor p21 protein expression, and induced apoptosis. APO10LA supplementation (10 mg/kg diet) for 24 weeks significantly reduced diethylnitrosamine-initiated, high fat diet (HFD)–promoted hepatic tumorigenesis (50% reduction in tumor multiplicity; 65% in volume) and lung tumor incidence (85% reduction) in C57Bl/6J mice. The chemopreventative effects of APO10LA were associated with increased hepatic SIRT1 protein and deacetylation of SIRT1 targets, as well as with decreased caspase-1 activation and SIRT1 protein cleavage. APO10LA supplementation in diet improved glucose intolerance and reduced hepatic inflammation [decreased inflammatory foci, TNFα, interleukin (IL)-6, NF-κB p65 protein expression, and STAT3 activation] in HFD-fed mice. Furthermore, APO10LA suppressed Akt activation, cyclin D1 gene, and protein expression and promoted PARP protein cleavage in transformed cells within liver tumors. Taken together, these data indicate that APO10LA can effectively inhibit HFD-promoted hepatic tumorigenesis by stimulating SIRT1 signaling while reducing hepatic inflammation. *Cancer Prev Res; 6(12); 1304–16. ©2013 AACR.*

Introduction

Primary liver cancer is the third leading cause of cancer deaths in the world (1, 2). Hepatocellular carcinoma (HCC) is the most common type of primary liver cancer accounting for 70% to 85% of cases (1, 2), with the rates twice as high in males as in females (1). The escalating morbidity and mortality of HCC trends parallel to the increasing prevalence of nonalcoholic fatty liver disease (NAFLD), a pathology that is observed in 75% to 100% of overweight and obese adults and children (3, 4). NAFLD prevalence increases with age (5) and can progress to the more severe form of NAFLD called nonalcoholic steatohepatitis (NASH). NASH is associated with insulin resistance, increased oxidative stress, induced inflammatory cytokine release, and can ultimately lead to cirrhosis and end-stage liver disease, including HCCs (6). Given the obesity epidemic, poor prognosis of HCC and its high mortality rate, the prevention of obesity/NAFLD through dietary means represents an important disease control strategy for preventing liver cancer.

Chronic liver inflammation, as displayed in NASH, plays a key role in enhancing liver tumorigenesis (6, 7). Previous animal studies showed that high fat diet (HFD) and obesity promote liver tumorigenesis by inducing chronic inflammation through the interleukin (IL)-6/STAT3 pathway, with STAT3-activated tumors being more aggressive in humans (6, 8–10). Sirtuin 1 (the mammalian ortholog of yeast Sir2; SIRT1) is a conserved NAD^+-dependent protein deacetylase expressed in various tissues including the liver (11). Mammalian SIRT1 has emerged as a key metabolic sensor linking nutrient signals to metabolic homeostasis

Authors' Affiliations: [1]Nutrition and Cancer Biology Laboratory, [2]Comparative Biology Unit, [3]Obesity and Metabolism Laboratory, Jean-Mayer United States Department of Agriculture Human Nutrition Research Center on Aging at Tufts University; and [4]Friedman School of Nutrition Science and Policy, Tufts University, Boston, Massachusetts

Note: Supplementary data for this article are available at Cancer Prevention Research Online (http://cancerprevres.aacrjournals.org/).

Corresponding Author: Xiang-Dong Wang, Nutrition and Cancer Biology Laboratory, Jean-Mayer United States Department of Agriculture Human Nutrition Research Center on Aging at Tufts University, 711 Washington Street, Room 514, Boston, MA 02111. Phone: 617-556-3130; Fax: 617-556-3344; E-mail: xiang-dong.wang@tufts.edu

doi: 10.1158/1940-6207.CAPR-13-0178

(11). SIRT1-mediated metabolic modulations have been revealed to protect against HFD-induced hepatic inflammation by ameliorating HFD-induced hepatic expression of IL-6 and TNFα (11–14). The potential mechanisms involved include modulations of NF-κB signaling (11–14) and AMP-activated protein kinase (AMPK) (11). More importantly, genetic overexpression of SIRT1 has been shown to protect mice from HFD-promoted hepatocarcinogenesis (14). These demonstrations raise an important question as to whether dietary compounds that can upregulate SIRT1 expression and/or activity may exhibit anti-inflammatory and anticarcinogenic effects.

Epidemiologic studies have established beneficial effects of lycopene-rich tomato and tomato products against various cancers (as reviewed in refs. 15–17). Although it remains to be determined as to whether lycopene is an important nutrient with health benefits, increasing *in vivo* and *in vitro* evidence support that lycopene has multifaceted biologic functions (15–17). These established biologic effects of lycopene include antioxidant functions, suppression of cell proliferation, anti-angiogenesis, and anti-inflammation (17–19). In regard to liver cancer risks, patients with NASH have been shown to have significantly reduced plasma lycopene (20), suggesting the potential interactions between low lycopene status and the development of liver diseases (20). Dietary lycopene has been shown to reduce the diethylnitrosamine (DEN) initiation of liver preneoplastic foci in rats (21). Our laboratory showed that lycopene supplementation can ameliorate DEN-initiated, HFD-promoted precancerous lesions in the liver (22). Apart from reducing hepatic tumorigenesis, lycopene supplementation has also been shown to inhibit experimental metastasis of injected human hepatoma cells in mice (19). However, our mechanistic understanding of how lycopene functions against tumorigenesis, specific ally HFD/obesity-related hepatic inflammation and tumorigenesis is far from complete.

We and others have recently shown that lycopene as a non-provitamin A carotenoid can be preferentially cleaved by the enzyme β-carotene 9′,10′-oxygenase (BCO2), and generate metabolites including apo-10′-lycopenal, apo-10′-lycopenol and apo-10′-lycopenoic acid (APO10LA; chemical structure in Supplementary Fig. S1; refs. 23, 24). Studies suggest that these metabolites may exhibit more important biologic roles than their parent compound lycopene (17, 25–28), providing the rationale to investigate BCO2-mediated vertebrate carotenoid metabolism and associated health outcomes. BCO2 is highly expressed in the liver and in other peripheral tissues (29). Modulating BCO2 expression can alter lipid metabolism, oxidative stress, and lycopene concentration in both hepatic and adipose tissue, as well as in plasma (30, 31). Interestingly, the single-nucleotide polymorphism (SNP) rs2115763 at the BCO2 locus was associated with elevated IL-18 concentration (32), a pro-inflammatory cytokine that correlated with diabetes and cardiovascular disease. Female variant allele carriers of a common SNP in the BCO2 gene can also have reduced fasting HDL cholesterol concentrations (32).

Recent investigations including our own show that lycopene metabolite APO10LA displays significant biologic activities (17). These activities include the transactivation of retinoid acid receptor elements (RARE; refs. 25, 28), the induction of retinoic acid receptor beta (RARβ; ref. 25), and the inhibition of lung cancer development (25). Other lycopene metabolites including apo-12′-lycopenal and apo-8′-lycopenal can also reduce cell proliferation in human prostate cancer DU145 cells (33) and inhibit metastatic behavior of human liver adenocarcinoma SK-Hep-1 cells (26), respectively. Intriguingly, we have recently revealed that APO10LA can upregulate the hepatic expression of SIRT1, decrease acetylation of SIRT1 downstream target, and inhibit hepatic steatosis in genetically induced obese (*ob/ob*) mice (27). However, whether APO10LA can upregulate SIRT1 signaling and ameliorate HFD-promoted liver inflammation and tumorigenesis remain to be explored.

The present study investigated the potential inhibitory effects of APO10LA against HFD-promoted hepatic tumorigenesis and elucidated, using both *in vitro* and *in vivo* models, the underlying mechanisms by which APO10LA exhibits these chemopreventative effects.

Materials and Methods

In vitro study—cell lines, reagents, and APO10LA treatment

The THLE-2 human immortalized liver cell line and HuH7 human liver cancer cell line were purchased from the American Type Culture Collection. These cell lines were not authenticated once received by our laboratory. Cells were cultured at 37°C in a humidified incubator containing 5% CO_2, in the "complete" bronchial epithelial cell growth medium (BEGM) supplemented with 10% FBS. The "complete-BEGM" incorporated the addition of Bullet kit CC3170 (Lonza), 5 ng/mL EGF, and 70 ng/mL phosphoethanolamine. A stock solution of APO10LA (20 mmol/L; BASF) was dissolved in tetrahydrofuran (THF; Sigma-Aldrich; containing 0.025% butylated hydroxytoluene as an antioxidant) and stored at −80°C. A working solution was prepared in the culture medium immediately before use. Using high-performance liquid chromatography (HPLC), we analyzed and recovered more than 95% of APO10LA in cell culture medium after 2 to 3 days of treatment. THLE-2 cells (3×10^5) were seeded in 60-mm plates coated with bovine serum albumin/collagen/fibronectin in 10% FBS-supplemented "completed-BEGM" medium for experiments. After overnight incubation, the cells were treated with increasing concentrations of APO10LA or vehicle (0.1% THF as control) in serum-free "completed-BEGM" medium for the indicated time. The cells were subsequently collected for analysis.

In vitro study—cell proliferation assay

THLE-2 cells were seeded at 5×10^3 cells per well and incubated overnight in 96-well plates in 10% FBS-supplemented "completed-BEGM" medium. Cells were subsequently treated with varying concentrations of APO10LA

in serum-free "completed-BEGM" medium for indicated time points. Cell proliferation was analyzed using the AQueous One Solution Cell Proliferation Assay Kit (Promega). All measurements were done in triplicate.

In vivo experiments—study design

The experimental protocol was adapted from a well-established animal model to study HCC pathogenesis (9, 34–37). All animal protocols were approved by the Institutional Animal Care and Use Committee at the JM-USDA Human Nutrition Research Center on Aging at Tufts University. Pregnant female C57Bl/6J mice were purchased from the Jackson Laboratories to generate male C57Bl/6J mice for this study. Male mice were acclimated to the standard laboratory chow (Harlan Laboratories), given water ad libitum, while kept on a 12-hour light/dark cycle in a controlled temperature and humidity room. Two-week-old mice were randomized to either be injected intraperitoneally (i.p.) with saline (−DEN arm) or with the well-established liver-specific carcinogen DEN (Sigma-Aldrich; +DEN arm) at a dosage of 25 mg/kg body weight as previously described (9). At 6 weeks of age, mice under the +DEN arm were randomized to either an obesogenic HFD (HFD+DEN; Bio-Serv; composition in Supplementary Table S1), in which 60% of energy is fat derived, or the same HFD supplemented with APO10LA (HFD+DEN+APO10LA; 10 mg/kg diet) for 24 weeks. Mice without DEN initiation were given the HFD only (HFD-DEN). All mice were given fresh diets every 2 to 3 days and maintained on their respective diets until the experiment was completed. Body weights of mice were recorded weekly. Mice were euthanized at 30 weeks of age by exsanguinations under deep anesthesia without fasting.

In vivo experiments—APO10LA treatment

The APO10LA used in this study was provided by Dr. Hansgeorg Ernst (BASF) with 99% purity and was incorporated directly into the diet to achieve a homogenous diet mixture. Diets with APO10LA were made every 2 to 4 weeks and were kept at −20°C (up to 4 weeks) or 4°C (<1 week) inside opaque boxes to avoid degradation of APO10LA. The APO10LA concentration and stability in the diet were evaluated as previously described (23, 25). APO10LA degradation was between 0.5 and 5% at −20°C or 4°C for 1 month and was less than 10% at room temperature for 3 days. The rationale for selecting this APO10LA dose was based on the reduced murine absorption of carotenoids (~1/10 of human absorption; refs. 25, 27, 38). An established equation is used to calculate the dosage equivalence for human consumption (39), which indicated that our APO10LA supplemented dose of 10 mg/kg diet is approximately equivalent to 0.36 mg APO10LA/day in a 60 kg adult man. A/J mice supplemented with the same APO10LA dose for 14 weeks resulted in a plasma APO10LA concentration of ~1.0 nmol/L (25). This amount is comparable to the sum of apo-lycopenals (1.9 nmol/L) but much lower than lycopene (1,089 ± 380 nmol/L) found in human plasma of individuals who had consumed tomato juice (with 21.8 mg lycopene/day) for 8 weeks (40). The APO10LA dose we used was about 20 times less than the average human dietary lycopene (~8 mg/d; ref. 16) and much lower than lycopene doses used in dietary supplements (15–30 mg/d).

In vivo experiments—glucose and insulin tolerance test

Mice underwent 6-hour fasts in 2 separate occasions that were 2 weeks apart and were injected with glucose (1 g/kg body weight; i.p.) or insulin (0.75 U/kg body weight; i.p.). Blood samples were collected from tail vein at different time points (0, 30, 60, 90, 120 minutes) post-glucose administration, and blood glucose was measured using a glucometer (LifeScan).

In vivo experiments—liver tumors quantification

Whole livers were removed from study mice posteuthanization. Surface liver tumors (tumor multiplicity) were counted by 2 investigators blinded to treatments, and the tumor diameters were measured with a caliper to calculate tumor volume. Tumor volume was calculated on the basis of the assumption that the tumor was spherical (volume $= 4/3\pi r^3$, where $r =$ diameter/2). Liver weights were recorded after removal of the intact gallbladder, and the liver was washed with saline for further processing. Large surface tumors were removed, snap-frozen in liquid nitrogen, and stored at −80°C. The right lobe of mouse liver was fixed in 10% buffered formalin solution (Thermo Fisher Scientific) and embedded in paraffin for serial sectioning and subsequent analysis by histologic methods. The remaining sections of liver were divided into smaller portions, snap-frozen in liquid nitrogen, and stored at −80°C.

In vivo experiments—histopathologic evaluation

Five-micrometer sections of formalin-fixed, paraffin-embedded liver tissue were stained with hematoxylin (H) and eosin (E) for histopathologic examination. Two independent investigators blinded to treatment groups examined the sections under light microscopy. Liver histopathology of nontumor areas was graded according to steatosis magnitude (both macro- and microvesicular) and the degree of liver inflammation severity as described previously (41, 42). Briefly, the degree of steatosis was graded 0–4 (grading 0 = <5%, 1 = 5%–25%, 2 = 26%–50%, 3 = 51%–75%, 4 >75%), based on the average percent of fat-accumulated hepatocytes per field at 100× magnification under H&E staining in 20 random fields. Inflammatory foci were evaluated by the number of inflammatory cell clusters in 20 random fields at 100× magnification, which mainly constitute mononuclear inflammatory cells. Mean foci per field was calculated and reported as inflammatory cell clusters per cm^2. Liver histopathology of the tumor areas was classified as hyperplasia, adenoma, and HCCs.

In vivo experiments—HPLC analysis

Hepatic APO10LA concentrations were measured by HPLC as previously described (23, 25). APO10LA was

quantified relative to the internal standard by determining peak areas calibrated against known amounts of standard.

Analysis for both *in vitro* and *in vivo* studies—RNA extraction and quantitative real-time PCR

Total RNA was extracted from THLE-2 cells and from frozen liver sections with TRIzol reagent (Invitrogen), as previously described (27). cDNA was prepared from the RNA samples using M-MLV reverse transcriptase (Invitrogen) and an automated thermal cycler PTC-200 (MJ Research). Quantitative real-time PCR (qRT-PCR) was carried out using FastStart Universal SYBR Green Master (ROX; Roche). Relative gene expression was determined using the $2^{-\Delta\Delta CT}$ method. Primer sequences are listed in Supplementary Table S2.

Analysis for both *in vitro* and *in vivo* studies—protein isolation and Western blotting

THLE-2 cells were lysed in cold whole-cell lysis buffer (25 mmol/L HEPES at pH = 7.5, 300 mmol/L NaCl, 1.5 mmol/L $MgCl_2$, 1 mmol/L EDTA, 10% glycerol, 1% Triton X-100) containing protease inhibitors. The THLE-2 cell lysates were centrifuged at 15,000 × *g* for 10 minutes at 4°C, and the supernatant was used. Tissue protein lysates were prepared by treating liver tissue with lysis buffer as described previously (27). The protein concentration of the supernatant was measured by the Coomassie Plus Protein Quantification Method (Thermo Fisher Scientific). For Western blotting, equal amounts of protein (30–50 μg for *in vitro* study and 50–100 μg for *in vivo* study) of each sample were boiled in reducing Laemmli sample buffer and resolved by 8% to 12% SDS-PAGE. Proteins were then transferred onto Immobilon-P membranes (Millipore), blocked with 5% non-fat milk in TBST buffer, and incubated with selected primary antibody. The following antibodies were used for Western blotting: acetylated NF-κB p65 (Lys310), AMPKα, Akt, cleaved PARP, NF-κB p65, phosphorylated-Akt (Ser473), phosphorylated-AMPKα (Thr172), phosphorylated-STAT3 (Tyr705), p21, STAT3, TNFα (Cell Signaling); IL-6 (R&D); acetylated-FoxO1, caspase-1, cyclin D1, FoxO1, and SIRT1 (Santa Cruz). Proteins were detected by a horseradish peroxidase–conjugated secondary antibody (Bio-Rad). The specific

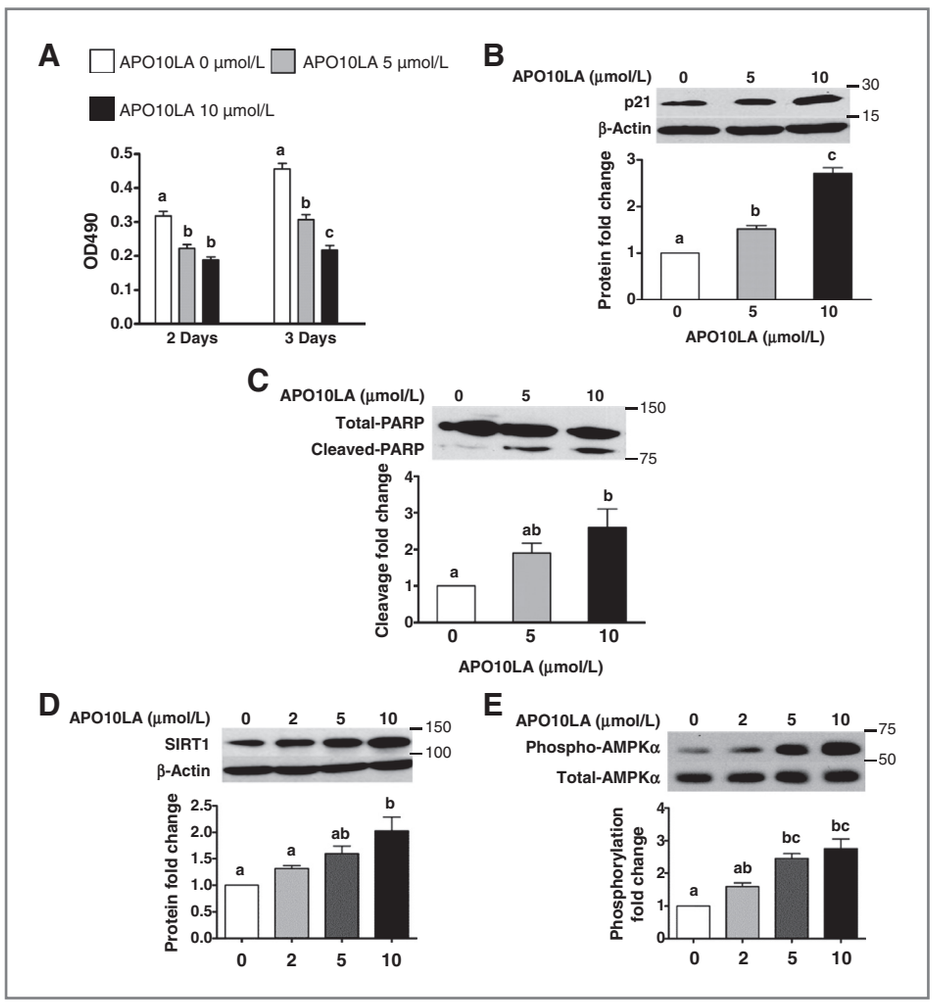

Figure 1. Effects of APO10LA treatments in THLE-2 cells. THLE-2 cells were plated and treated with indicated concentration of APO10LA for 2 or 3 days as described in Materials and Methods. Protein expression in cell lysates were analyzed by Western blotting and β-actin was used as loading control unless specified otherwise. A, cell proliferation. B, p21 protein level. C, PARP cleavage (PARP as loading control). D, SIRT1 protein level. E, AMPKα (Thr172) phosphorylation (AMPKα as loading control). Representative Western blot analyses of 3 independent experiments are shown, and all treatments were conducted in triplicates. For B–E, the data reflect 2-day APO10LA treatments. Data presented in different letter superscripts represent $P \leq 0.05$. All fold changes normalized to APO10LA = 0 μmol/L.

bands were visualized by a SuperSignal West Pico Chemiluminescent Substrate Kit (Pierce) according to the manufacturer's instructions. Anti-actin antibody (Sigma-Aldrich) was used to detect β-actin for loading normalization of some proteins. Intensities of protein bands were quantified using GS-710 Calibrated Imaging Densitometer (Bio-Rad).

Analysis for both *in vitro* and *in vivo* studies—statistical analysis

For *in vitro* study, GraphPad Prism (GraphPad Software) was used to conduct the statistical analysis, and resulting values were expressed as means ± SEM. Group means were compared using one-way ANOVA analysis with Bonferroni adjustments for multiple comparisons. For *in vivo* study, SAS 9.3 software was used to conduct the statistical analysis. Student *t* test was used to test for the differences between the following comparisons: (i) HFD-DEN and HFD+DEN and (ii) HFD+DEN and HFD+DEN+APO10LA. *P* value was set at 0.05 for the comparisons to reach statistical significance.

Results

APO10LA reduced cell proliferation and induced apoptosis in liver cells

To elucidate the potential molecular targets of APO10LA, we first conducted an *in vitro* study using THLE-2 cells (primary normal liver cells transformed by SV40 large T antigen infection), and the HuH7 human liver cancer cell line. APO10LA treatments on THLE-2 significantly reduced cell proliferation (30%–50% reduction) in a dose-dependent manner (Fig. 1A). Similar effects were observed in HuH7 cells (data not shown). As APO10LA may function as a retinoic acid (RA) analog (Supplementary Fig. S1 for chemical structure) and transactivates RAREs (25, 28), we examined p21 protein expression, an RA-inducible protein that inhibits cell-cycle progression (43). APO10LA treatments dose dependently upregulated p21 protein expression (Fig. 1B) and induced PARP protein cleavage in THLE-2 cells (Fig. 1C), indicating the induction of cell apoptosis. Furthermore, APO10LA treatments dose dependently upregulated SIRT1 protein expression (Fig. 1D) but did not alter

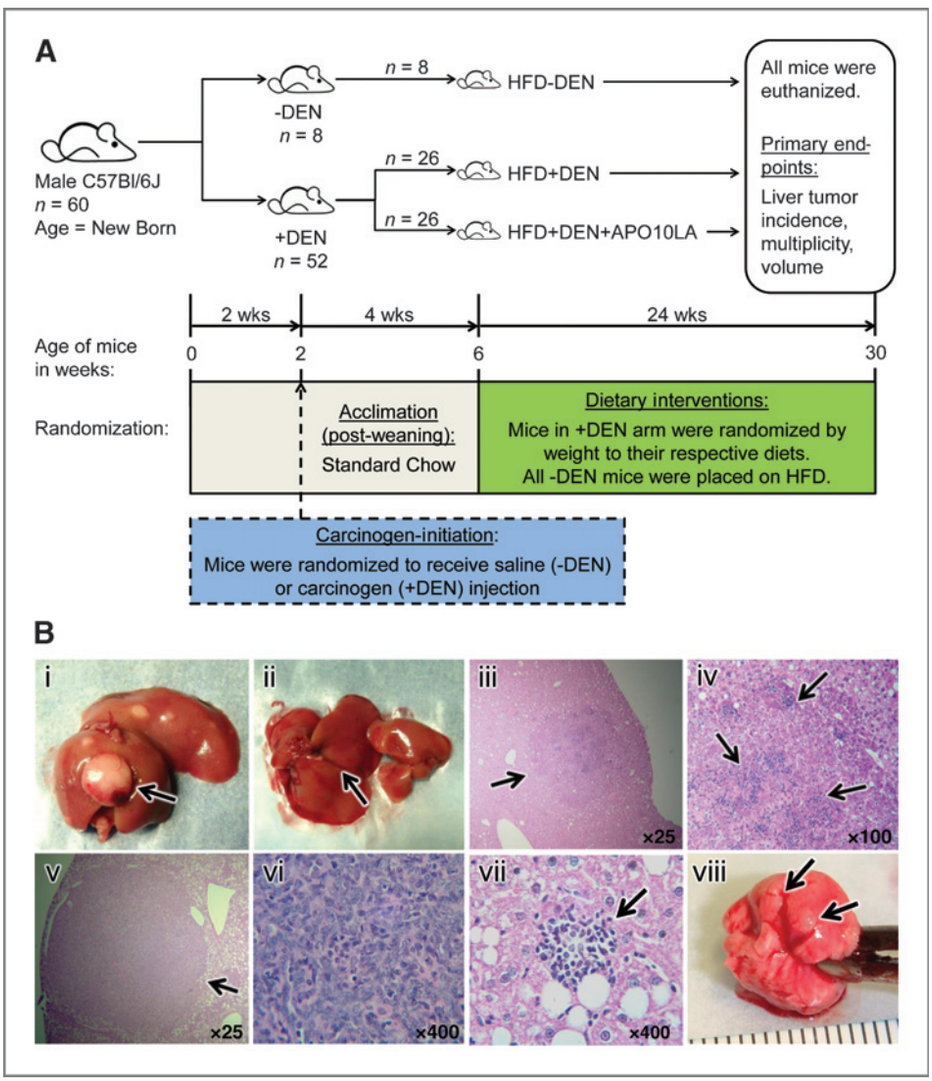

Figure 2. *In vivo* study design, gross, and histopathology of liver tumors, inflammation, and lung tumor. A, *in vivo* study design. B, representative picture or light micrograph of livers from HFD+DEN or HFD+DEN+APO10LA. B, i, livers from HFD+DEN with tumors (arrow). ii, livers from HFD+DEN+APO10LA with tumors (arrow). iii, H&E-stained hepatic adenoma (arrow) at 25×. iv, H&E-stained hepatic adenoma with inflammatory cell infiltration (arrows) at 100×. v, H&E-stained HCCs at 25×. vi, H&E-stained poorly differentiated (discohesive, pleomorphic, anaplastic, giant) HCC at 400×. vii, H&E-stained hepatic inflammatory foci in the nontumor region at 400×. viii, lung surface tumors (arrows).

Sirt1 mRNA level in THLE-2 cells (data not shown). As SIRT1 modulates hepatic metabolic homeostasis, in part, through AMPK activation (11), we examined AMPKα phosphorylation in THLE-2 cells and found that APO10LA-induced upregulation of SIRT1 was associated with increased AMPKα phosphorylation (Fig. 1E).

APO10LA inhibited DEN-initiated, HFD-promoted hepatic tumorigenesis and reduced glucose intolerance in mice without altering body/liver weights

We conducted a dietary intervention study with APO10LA at 10 mg/kg diet in a DEN-initiated, HFD-promoted liver cancer model with C57Bl/6J male mice for 24 weeks (Fig. 2A: study design). This is a well-established animal model to study HCC pathogenesis (9, 34–37). As expected, liver tumors failed to develop in the absence of DEN-injection (HFD-DEN; Table 1). Similar to the results described by Park and colleagues (9), DEN-initiation resulted in visible and multiple surface liver tumors in HFD-fed mice [Fig. 2B (i) and (ii)]. H&E staining of formalin-fixed, paraffin-embedded liver tissues showed the development of both hepatic adenoma and HCCs in C57Bl/6J mice [Fig. 2B (iii)–(vi)], with infiltration of inflammatory cells within both nontumor and tumor regions [Fig. 2B (iii), (iv), (vi)]. APO10LA supplementation in diet significantly decreased the hepatic surface tumor multiplicity [by 50%; Table 1; Fig. 2B (i) and (ii)], and volume (by 65%; Table 1). All DEN-injected mice developed liver tumors, and APO10LA did not alter liver tumor incidence (Table 1). Interestingly, lung tumors developed in 26% of HFD+DEN mice [Fig. 2B (viii); Table 1], and APO10LA supplementation significantly decreased lung tumor incidence to less than 5% (Table 1). Final mean body and liver weights did not differ between all 3 groups (Table 1). Body weights were comparable to the C57Bl/6J diet-induced obesity phenotype described by The Jackson Laboratory (44) and Park and colleagues (9), where mice were placed on a diet with 60% of energy from fat for 20 to 26 weeks. All groups of mice in this present study exhibited the same degree of mortality (Table 1). However, APO10LA supplementation significantly reduced glucose intolerance (Table 1; Supplementary Fig. S2) without altering global insulin resistance, as compared to HFD+DEN (data not shown). Hepatic APO10LA concentration was 0.3 ± 0.1 pmol/g liver in APO10LA-supplemented mice and was not detectable in mice without supplementation (Table 1).

APO10LA reduced the number of hepatic inflammatory foci and expression of pro-inflammatory biomarkers

All three groups exhibited the same degree of hepatic steatosis in the nontumor regions (Table 1). HFD+DEN displayed a significant increase in hepatic inflammatory foci as compared to HFD-DEN mice without DEN injection. APO10LA supplementation in diet significantly reduced the number of hepatic inflammatory foci (by 65%; Table 1) in the nontumor regions, as compared to HFD+DEN. Supplementation with APO10LA did not alter the mRNA expression of *Tnfα*, *Il-6*, and *Il-1β* as compared to HFD+DEN (data not shown). Nevertheless, APO10LA significantly reduced hepatic pro-inflammatory biomarkers including TNFα (38%; Fig. 3A), IL-6 (by 50%; Fig. 3B), NF-κB p65 (by 40%; Fig. 3C) protein expression, caspase-1 cleavage (by 55%; Fig. 3D), and STAT3 phosphorylation (Tyr705; by 55%; Fig. 3E) in the overall liver tissue, as compared to HFD+DEN. NF-κB p65 protein expression

Table 1. Primary outcomes

	Study group		
	HFD-DEN	**HFD+DEN**	**HFD+DEN+APO10LA**
Animal number (*n*)	8	26	26
Mortality (no. of animals)	1†	2^{‡,a}	2^{a}
Liver tumor			
Incidence, %	0‡	100$^{\dagger a}$	100^{a}
Multiplicity, #	0‡	14.6 ± 1.9$^{\dagger a}$	7.6 ± 1.0^{b}
Volume, mm^3	0‡	306.2 ± 113.2$^{\dagger a}$	101.8 ± 33.9^{b}
Lung tumor incidence, %	0‡	26$^{\dagger a}$	4^{b}
Final body weight, g	52.9 ± 1.4†	50.9 ± 0.6$^{\dagger a}$	50.5 ± 1.0^{a}
Liver weight, g	4.9 ± 0.1†	4.8 ± 0.1$^{\dagger a}$	4.6 ± 0.1^{a}
Hepatic steatosis score [median (range)]	2 (1–2)†	2 (1–3)$^{\dagger a}$	2 (0–2)^{a}
Liver inflammatory foci (number/cm^2)	0 ± 0‡	1.7 ± 0.5$^{\dagger a}$	0.6 ± 0.2^{b}
Hepatic APO10LA (pmol/g of liver)	ND	ND	0.3 ± 0.1
Glucose intolerance (AUC)	796.5 ± 64.5†	797.0 ± 36.5$^{\dagger a}$	600.0 ± 18.4^{b}

NOTE: Data shown are mean ± SEM unless otherwise indicated. Different letter or symbol superscripts represent $P \leq 0.05$ for comparisons between HFD+DEN and HFD+DEN+APO10LA (letters) or HFD+DEN and HFD-DEN (symbols). See Supplementary Fig. S2 for the graphical presentation of glucose tolerance test.

Abbreviation: ND, not detected.

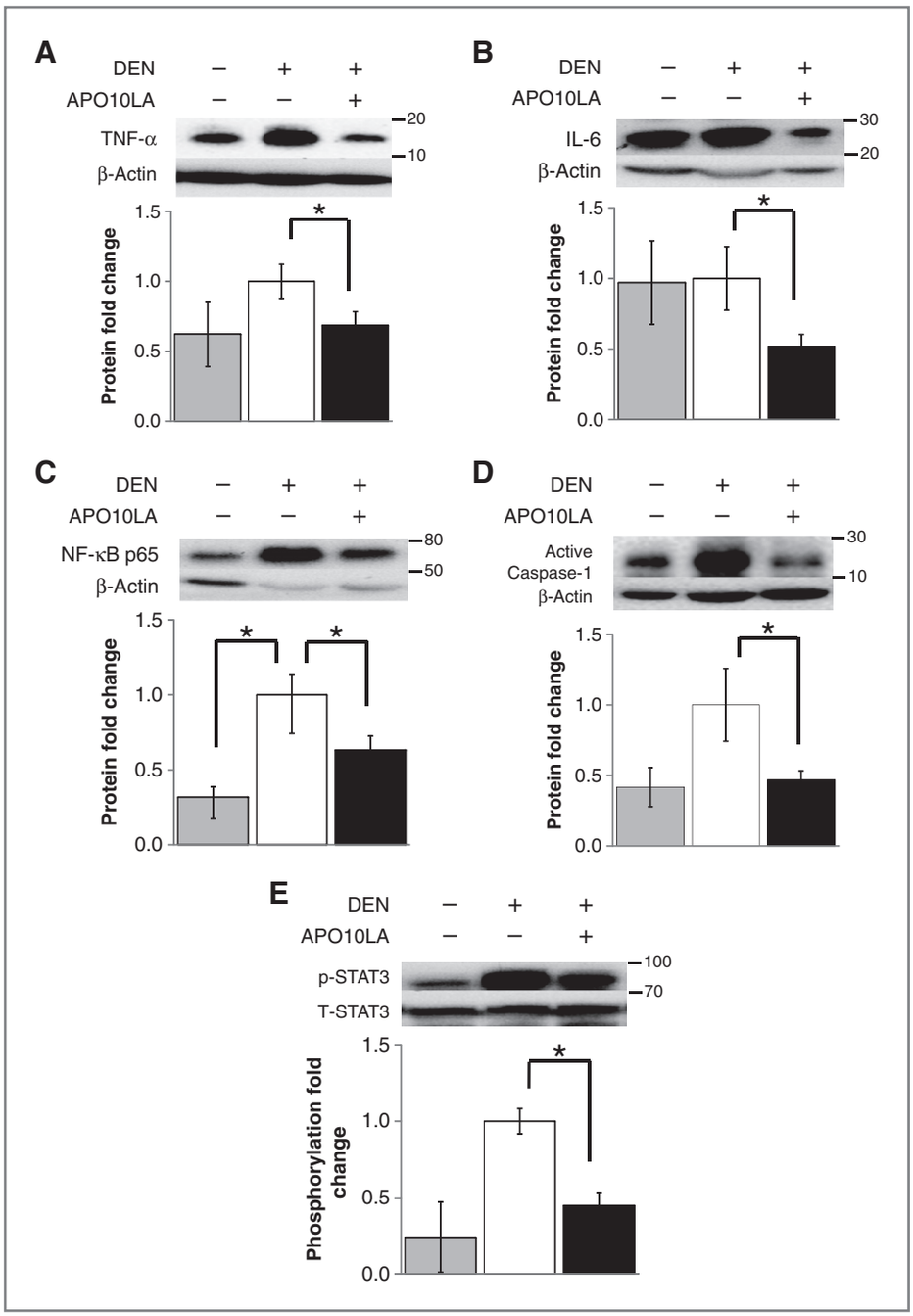

Figure 3. Effects of APO10LA supplementation on hepatic pro-inflammatory biomarkers. *In vivo* study design. Protein expression in liver lysates (HFD-DEN, $n = 6$; HFD+DEN and HFD+DEN+APO10LA, $n = 22$) were analyzed by Western blotting and β-actin was used as loading control unless specified otherwise. Graphical representation of fold changes in: A, TNFα; B, IL-6; C, NF-κB p65; D, active caspase-1; E, STAT3 (Tyr705) phosphorylation (STAT3 as loading control). Representative Western blot analyses with 1 sample per group are shown. Fold changes normalized to HFD+DEN. Data shown are mean ± SEM. *, $P \leq 0.05$; **, $P \leq 0.01$ for comparisons between HFD+DEN and HFD+DEN+APO10LA or HFD+DEN and HFD-DEN.

was correlated with IL-6 protein expression ($R^2 = 0.35$; $P < 0.001$) and liver tumor volume ($R^2 = 0.36$; $P = 0.018$), whereas IL-6 protein expression was correlated with TNFα protein expression ($R^2 = 0.39$; $P = 0.010$) and SIRT1 cleavage ($R^2 = 0.38$; $P = 0.012$). The HFD+DEN group also had a 2-fold induction of NF-κB p65 protein expression as compared to the HFD-DEN group (Fig. 3C). None of these modulations were observed within the liver tumor regions between HFD+DEN and HFD+DEN+APO10LA groups (data not shown).

Reduction in HFD-promoted hepatic tumorigenesis by APO10LA was associated with increased hepatic SIRT1 protein, deacetylation of FoxO1 and NF-κB, and AMPKα phosphorylation

APO10LA supplementation did not alter the mRNA expression of *Sirt1* as compared to HFD+DEN (data not shown). However, as compared to HFD+DEN, APO10LA significantly increased hepatic SIRT1 protein expression (by 50%; Fig. 4A) to a level that was comparable to HFD-DEN and induced the deacetylation of SIRT1 direct targets, which

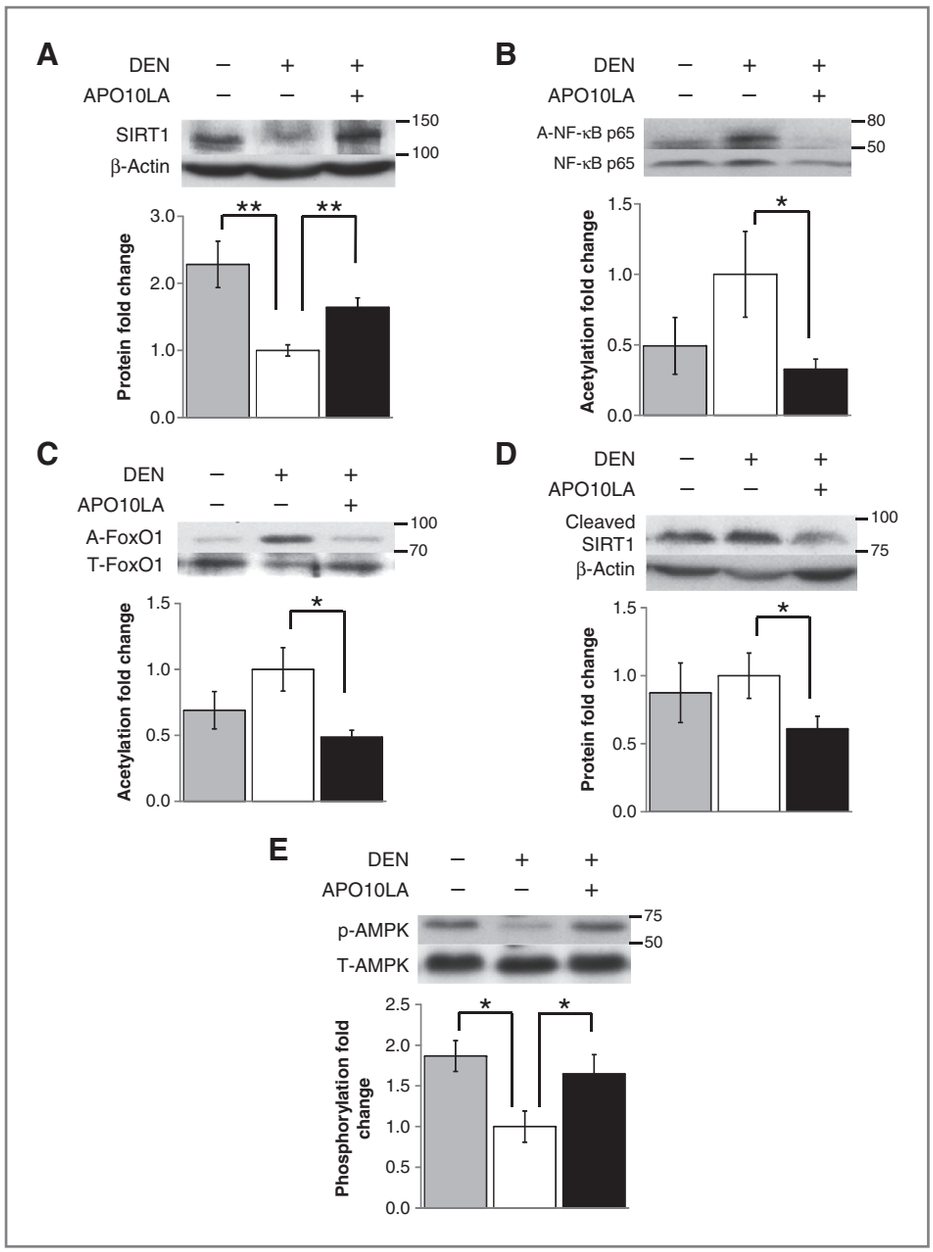

Figure 4. Modulations in hepatic SIRT1 expression and its deacetylation targets as well as AMPKα phosphorylation by APO10LA. Protein expression in liver lysates (HFD-DEN, $n = 6$; HFD+DEN and HFD+DEN+APO10LA, $n = 22$) were analyzed by Western blotting and β-actin was used as loading control unless specified otherwise. Graphical representation of fold changes in: A, SIRT1; B, NF-κB p65 (Lys310) acetylation (NF-κB p65 as loading control); C, FoxO1 acetylation (FoxO1 as loading control); D, cleaved SIRT1. E, AMPKα (Thr172) phosphorylation (AMPKα as loading control). Representative Western blot analyses with 1 sample per group are shown. Fold changes normalized to HFD+DEN. Data shown are mean ± SEM. *, $P \leq 0.05$ for comparisons between HFD+DEN and HFD+DEN+APO10LA or HFD+DEN and HFD-DEN.

included NF-κB p65 (Lys310; by 67%; Fig. 4B) and FoxO1 (by 50%; Fig. 4C) in the overall liver tissue. These observations were associated with the significant decrease in hepatic SIRT1 protein cleavage (by 40%; Fig. 4D) and with increased AMPKα phosphorylation (by 65%; Fig. 4E). Hepatic SIRT1 protein expression was inversely correlated with NF-κB p65 protein expression ($R^2 = -0.32$; $P = 0.048$), NF-κB p65 acetylation ($R^2 = -0.40$; $P = 0.007$), and SIRT1 protein cleavage ($R^2 = -0.36$; $P = 0.023$). Hepatic AMPKα phosphorylation was also inversely correlated with liver tumor numbers ($R^2 = -0.41$; $P = 0.007$) and TNFα protein expression ($R^2 = -0.51$; $P < 0.001$). DEN initiation in HFD+DEN had a significant reduction in hepatic SIRT1 protein expression (by 60%; Fig. 4A) and AMPKα phosphorylation (by 50%; Fig. 4E), as compared to HFD-DEN. None of these modulations were observed within the liver tumor regions between HFD+DEN and HFD+DEN+APO10LA groups (data not shown).

APO10LA induced PARP cleavage, suppressed Akt phosphorylation and cyclin D1 protein expression within the liver tumor region

APO10LA supplementation significantly reduced Akt phosphorylation (Ser473; by 45%; Fig. 5A) within the liver tumor region, as compared to HFD+DEN. This APO10LA-dependent phenomenon was accompanied with the

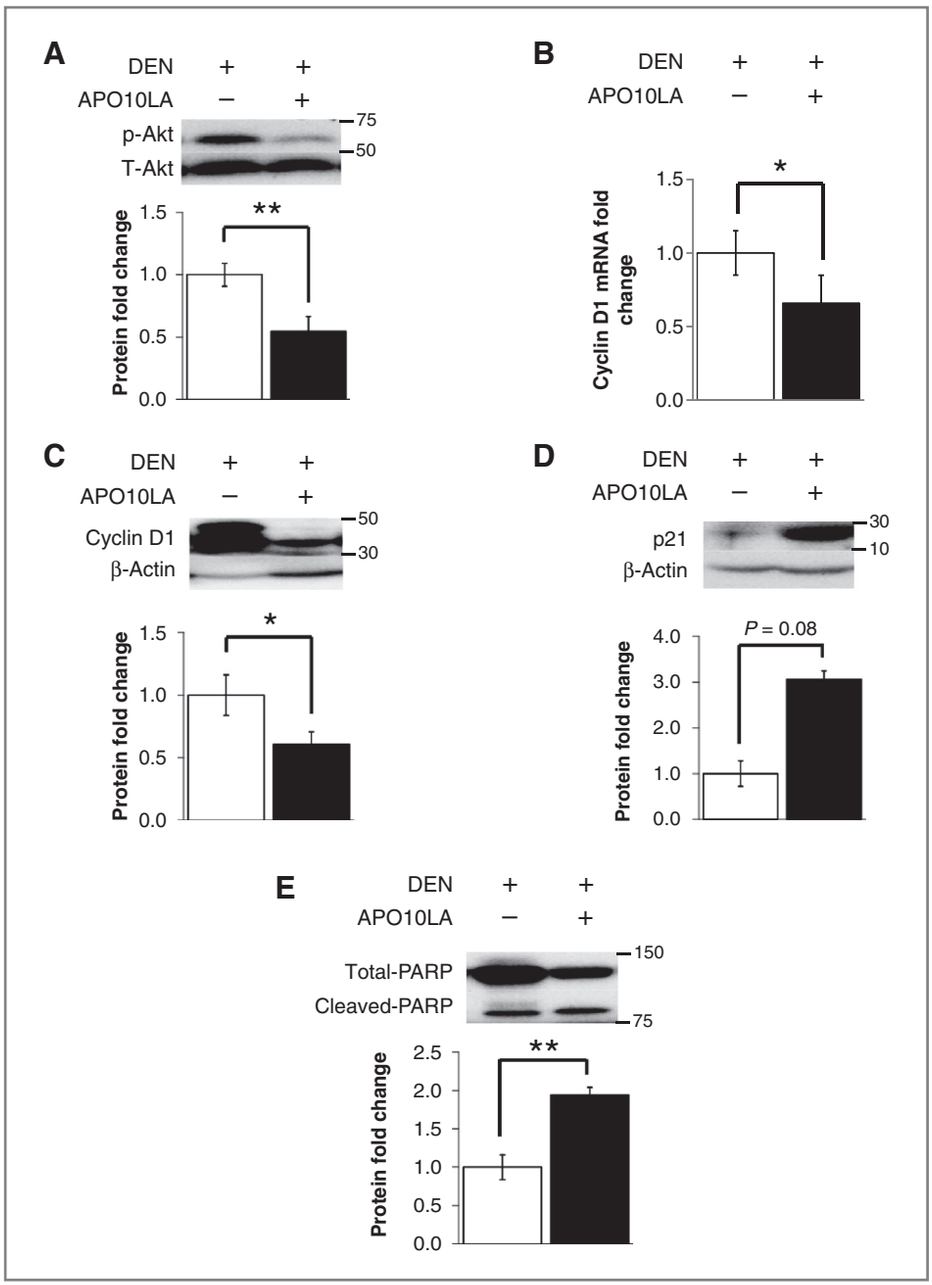

Figure 5. Effects of APO10LA on biomarkers involved in cell proliferation and apoptosis in liver tumors. mRNA from liver tumors ($n = 10$–12 per group) were analyzed by RT-PCR. Protein expression in liver tumor lysates ($n = 10$–12 per group) were analyzed by Western blotting and β-actin was used as loading control unless specified otherwise. Graphical representation of fold changes in: A, Akt (Ser473) phosphorylation (total Akt as loading control); B, cyclin D1 mRNA; C, cyclin D1 protein expression; D, p21 protein expression; E, PARP cleavage (PARP as loading control). Representative Western blot analyses with 1 sample per group are shown. Fold changes normalized to HFD+DEN. Data shown are mean ± SEM. *, $P \leq 0.05$; **, $P \leq 0.01$ for comparisons between HFD+DEN and HFD+DEN+APO10LA.

significant reduction in both cyclin D1 gene (by 31%; Fig. 5B) and protein expression (by 39%; Fig. 5C), as well as a nonsignificant upregulation of p21 protein expression (by 207%; $P = 0.08$; Fig. 5D) in tumor regions, indicating suppression in cancer cell proliferation. Cyclin D1 protein expression was correlated with Akt phosphorylation ($R^2 = 0.45$; $P = 0.045$) in liver tumors, glucose intolerance ($R^2 = 0.72$; $P = 0.048$), and with liver tumor numbers ($R^2 = 0.43$; $P = 0.061$) that almost reached statistical significance. APO10LA also significantly induced PARP protein cleavage (by 94%; Fig. 5E) within the tumor region as compared to HFD+DEN, suggesting the induction of apoptosis. All these modulations were specific to the liver tumor regions and were not observed within the overall liver tissue between HFD+DEN and HFD+DEN+APO10LA (data not shown).

Discussion

The present study provides the novel insight that APO10LA, a metabolite generated by the BCO2 cleavage enzyme from the non-provitamin A carotenoid lycopene, can inhibit HFD-induced liver inflammation and HFD-promoted liver tumorigenesis. Previous studies with

murine models and human cell lines lacking BCO2 enzyme showed that supplementation or treatment of non-provitamin A carotenoids can alter lipid metabolism and induce oxidative stress (30). SNP at the BCO2 locus was associated with elevated pro-inflammatory IL-18 in humans (32). This present study shows that APO10LA as a BCO2 cleavage product of lycopene has strong biologic activities and may function as an effective chemopreventative agent against HCC influenced by inflammation and metabolic syndrome. Our results support the notion that enzymatic cleavage products of non-provitamin A carotenoids may have more important biological roles than their parent compounds. A gene–diet interaction with respect to human health and disease may exist between the BCO2 enzyme and dietary carotenoids. Apart from endogenous synthesis, it is important to note that apo-lycopenoids do exist in dietary plant foods (40) and can be produced by nonspecific oxidation of carotenoids (45). As apo-lycopenals in human plasma can originate from diet and human metabolism (40), our present study can thus evaluate the potential biologic effects of lycopene metabolites derived from both dietary sources and *in vivo* metabolism. We have previously shown that tomato extract supplementation was more protective against HFD-induced hepatic inflammation than lycopene (22). Clearly, further investigations are needed to examine whether these dietary tomato-derived apo-carotenoids can provide protective effects against chronic diseases in humans.

In the present *in vivo* study, the hepatic concentration of APO10LA was in picomolar range (Table 1), which is markedly lower than hepatic lycopene concentration in rats (7.5–17.6 nmol/g liver; ref. 22) and in humans (0.1–20.7 nmol/g liver; ref. 46). However, the effective APO10LA concentrations to induce SIRT1 protein expression *in vitro* were between 2 and 10 μmol/L, which are higher than the reported human plasma lycopene concentration (50–900 nmol/L; ref. 15). Consistent with our previous studies using APO10LA (25, 47), we found that the intracellular APO10LA concentration was below detection level. In our previous *in vitro* study, A549 cells treated with 1 μmol/L of β-cryptoxanthin resulted in intracellular β-cryptoxanthin levels of 0.39 ng/10^6 cells (~0.04 μmol/L on the basis of cell volume; ref. 48). The absence of intracellular APO10LA could be due to the low carotenoids uptake in cell culture study, as well as further "leakage" of carotenoids during cell-washing procedures to avoid potential carotenoids contamination in cell membrane. Another study from our laboratory showed that dietary lycopene is better accumulated in tissue than in plasma (49). This may explain why the effective APO10LA concentration to induce SIRT1 was much higher than plasma concentration. In addition, we believe that the APO10LA supplemented dosage used in our study is physiologically relevant to the biologic effects of lycopene metabolites derived from both dietary sources and *in vivo* metabolism.

The chemopreventative effects of APO10LA showed in this investigation were associated with the reduction in hepatic inflammatory foci [Table 1; Fig. 2B (vii)], hepatic protein expression of TNFα, IL-6, and NF-κB p65, and the decreased activation of the oncogenic transcription factor STAT3 (Fig. 3). Moreover, reduction in NF-κB p65 protein in response to APO10LA supplementation was significantly correlated with decreased liver tumor volume and IL-6 expression. These results support the concept that obesity promotes liver tumorigenesis through IL-6/STAT3 activation (6, 9) and that APO10LA can reduce HFD-promoted liver inflammation and tumorigenesis.

Consistent with anti-inflammatory and chemopreventative actions, a key observation of this study is that APO10LA supplementation induced SIRT1 protein expression and increased deacetylation of SIRT1 targets (NF-κB p65 and FoxO1; Fig. 4A–C). SIRT1 has been shown to play a protective role against HFD-promoted hepatic steatosis, inflammation, and most recently hepatocarcinogenesis (11–14). It is proposed that SIRT1 attenuates hepatic protein expression of IL-6 and TNFα through deacetylation and/or reduced expression of NF-κB p65 (11–14, 50). Indeed, in the present study, SIRT1 protein expression was inversely correlated with both the NF-κB p65 acetylation and protein expression (Figs. 4A and B and 3C). SIRT1 protein level was also restored by APO10LA to HFD-DEN levels (Fig. 4A). Interestingly, APO10LA-induced hepatic SIRT1 protein expression occurred without changes in *Sirt1* mRNA levels, suggesting a posttranslational modification of SIRT1. Chalkiadaki and colleagues showed that HFD can stimulate SIRT1 protein cleavage by caspase-1 activation, leading to the reduction in SIRT1 deacetylation capacity (51). Caspase-1 is a downstream effector of the NLRP3 (NACHT, LRR and PYD domains-containing protein-3) inflammasome, a pro-inflammatory scaffolding complex that can activate the NF-κB–inducing cytokine IL-1β (52). The inflammasome is activated in the liver by HFD and obesity (52, 53), and AMPK activation by phosphorylation can attenuate this stimulation (52, 53). We found that APO10LA ameliorated HFD-induced activation of caspase-1 (Fig. 3D). Importantly, the APO10LA-mediated reduction in caspase-1 activation was significantly associated with reduced SIRT1 cleavage (Fig. 4D) and increased AMPK phosphorylation (Fig. 1E and 4E). Together, these findings suggest that APO10LA can interrupt the vicious cycle of HFD-promoted upregulation of NF-κB p65 signaling, escalation in inflammasome function, and reduction in SIRT1 signaling, thus delivering protection against this induced hepatic tumorigenesis. Further investigations with SIRT1-knockout mice are currently ongoing in our laboratory.

Increased Akt activation in transformed cells of human liver tumors is a risk factor for early disease recurrence (i.e., tumor growth, progression, invasion, and metastasis promotion; ref. 54). PI3K/Akt signaling in human HepG2 hepatoma cells plays a key role in basal cell proliferation that correlates with increased cyclin D1 (55) and in insulin growth factor receptor–mediated DNA replication (55). Small molecules that abrogate Akt phosphorylation in human HCC cell lines caused irreversible growth arrest and apoptosis (56), indicating the importance of Akt-mediated

signaling for the growth and survival of transformed cells within liver tumors. In the present study, APO10LA significantly reduced hepatic surface tumor volume by 65% (Table 1). Analysis of liver tumor regions revealed that this APO10LA-dependent tumor volume reduction was associated with suppressed Akt phosphorylation (Fig. 5A), attenuated cyclin D1 gene and protein expression (Fig. 5B and C), upregulated p21 protein expression (Fig. 5D), and induced PARP protein cleavage (Fig. 5E), as compared to HFD+DEN. These APO10LA-dependent modulations in biomarkers of cell proliferation and apoptosis were supported by our *in vitro* results (Fig. 1), thus providing a potential mechanism by which APO10LA may reduce liver tumorigenesis. We and others also showed that APO10LA may function as an RA analog to transactivate RAREs (25, 28) and induce RARβ expression *in vitro* (25, 28), therefore providing an alternative mechanism by which APO10LA may inhibit proliferation and promote apoptosis of transformed cells. Intriguingly, the chemical structure of APO10LA is also similar to acyclic RA (Supplementary Fig. S1), which has recently been shown to inhibit cyclin D1 expression and prevent hepatic fibrosis and HCC development (57).

Impaired glucose tolerance and insulin resistance are associated with human NAFLD (58), NASH (59), and are risk factors that can mediate the effects of obesity-induced inflammation (6, 59). Park and colleagues observed that obese mice bearing liver tumors were glucose intolerant and hyperinsulinemic when compared to lean mice bearing liver tumors (9). We asked whether tumor-bearing *per se* was associated with liver inflammation and glucose intolerance. The presence of liver tumors in our HFD-fed mice was associated with increased hepatic inflammation (Table 1; Fig. 3), but HFD-feeding regardless of liver tumor–bearing promoted glucose intolerance (Table 1), as compared to the lean chow-fed C57Bl/6J mice described by The Jackson Laboratory (44) and Park and colleagues (9). Importantly, APO10LA supplementation significantly reduced these pathologies (Table 1) without altering global insulin resistance. NF-κB signaling has been associated with glucose intolerance (6, 59). HFD-fed mice lacking the NF-κB–activating kinase IκB kinase β (*Ikk*β) in hepatocytes retained liver insulin sensitivity but developed insulin resistance in muscle and fat (6, 59). HFD-fed mice lacking *Ikk*β in myeloid cells, however, retained global insulin responsiveness and were protected from obesity-induced insulin resistance (6, 59). Subsequent research is required to investigate whether APO10LA supplementation might be predominately altering NF-κB signaling in myeloid cells.

Metastasis results in 90% of cancer-related fatalities, and extrahepatic metastasis of HCC occurs primarily in lungs of humans and mice (9, 34–37). In this study, APO10LA supplementation significantly decreased lung tumor incidence to less than 5% of mice, as compared to 26% in HFD+DEN [Fig. 2B (viii); Table 1]. This result supports our previous *in vivo* findings in A/J mice that APO10LA is a potential chemopreventive agent against lung tumorigenesis (25). DEN is a liver-specific procarcinogen in C57Bl/6 mice, and previous histologic studies observed pulmonary metastatic foci in mice bearing DEN-induced liver cancer (9, 34–37, 60). Thus, it is possible that APO10LA can inhibit HCC multiplicity, volume, as well as metastasis to the lungs. Previous studies showed that lycopene metabolites have antimetastatic effects in human liver adenocarcinoma SK-Hep-1 cells (26). Recently, we observed that APO10LA is effective at inhibiting migration and invasion of both cancer and endothelial cells by suppressing actin remodeling and ruffling/lamellipodia formation (B. Miao and X.D. Wang, unpublished data), indicating anti-angiogenesis as a potential mechanism for APO10LA chemopreventative properties.

Disclosure of Potential Conflicts of Interest

No potential conflicts of interest were disclosed.

Disclaimer

Any opinions, findings, conclusions, and recommendations expressed in this publication are those of the author(s) and do not necessarily reflect the views of the sponsors.

Authors' Contributions

Conception and design: B.C. Ip, K.-Q. Hu, D.E. Smith, M.S. Obin, L.M. Ausman, X.-D. Wang

Development of methodology: B.C. Ip, K.-Q. Hu, D. Liu, D.E. Smith, L.M. Ausman, X.-D. Wang

Acquisition of data (provided animals, acquired and managed patients, provided facilities, etc.): B.C. Ip, K.-Q. Hu, D. Liu, D.E. Smith, X.-D. Wang

Analysis and interpretation of data (e.g., statistical analysis, biostatistics, computational analysis): B.C. Ip, K.-Q. Hu, D. Liu, D.E. Smith, L.M. Ausman, X.-D. Wang

Writing, review, and/or revision of the manuscript: B.C. Ip, K.-Q. Hu, D. Liu, D.E. Smith, M.S. Obin, L.M. Ausman, X.-D. Wang

Administrative, technical, or material support (i.e., reporting or organizing data, constructing databases): B.C. Ip, K.-Q. Hu, D. Liu, X.-D. Wang

Study supervision: X.-D. Wang

Acknowledgments

The authors thank Dr. Hansgeorg Ernst (Fine Chemicals and Biocatalysis Research, BASF) for providing APO10LA.

Grant Support

The study was supported by the NIH grant CA104932 (X.-D. Wang) and USDA/ARS grant 1950-51000-074S (X.-D. Wang).

The costs of publication of this article were defrayed in part by the payment of page charges. This article must therefore be hereby marked *advertisement* in accordance with 18 U.S.C. Section 1734 solely to indicate this fact.

Received May 14, 2013; revised September 18, 2013; accepted September 22, 2013; published OnlineFirst October 1, 2013.

References

1. Siegel R, Naishadham D, Jemal A. Cancer statistics, 2012. CA Cancer J Clin 2012;62:10–29.

2. Forner A, Llovet JM, Bruix J. Hepatocellular carcinoma. Lancet 2012;379:1245–55.

3. Page JM, Harrison SA. NASH and HCC. Clin Liver Dis 2009;13:631–47.
4. Baffy G, Brunt EM, Caldwell SH. Hepatocellular carcinoma in non-alcoholic fatty liver disease: an emerging menace. J Hepatol 2012;56: 1384–91.
5. Clark JM. The epidemiology of nonalcoholic fatty liver disease in adults. J Clin Gastroenterol 2006;40:S5–10.
6. Sun B, Karin M. Obesity, inflammation, and liver cancer. J Hepatol 2012;56:704–13.
7. Hill-Baskin AE, Markiewski MM, Buchner DA, Shao H, DeSantis D, Hsiao G, et al. Diet-induced hepatocellular carcinoma in genetically predisposed mice. Hum Mol Genet 2009;18:2975–88.
8. Wang Y, Ausman LM, Greenberg AS, Russell RM, Wang XD. Nonalcoholic steatohepatitis induced by a high-fat diet promotes diethylnitrosamine-initiated early hepatocarcinogenesis in rats. Int J Cancer 2009;124:540–6.
9. Park EJ, Lee JH, Yu GY, He G, Ali SR, Holzer RG, et al. Dietary and genetic obesity promote liver inflammation and tumorigenesis by enhancing IL-6 and TNF expression. Cell 2010;140:197–208.
10. He G, Yu GY, Temkin V, Ogata H, Kuntzen C, Sakurai T, et al. Hepatocyte IKKbeta/NF-kappaB inhibits tumor promotion and progression by preventing oxidative stress-driven STAT3 activation. Cancer Cell 2010;17:286–97.
11. Houtkooper RH, Pirinen E, Auwerx J. Sirtuins as regulators of metabolism and healthspan. Nat Rev Mol Cell Biol 2012;13:225–38.
12. Pfluger PT, Herranz D, Velasco-Miguel S, Serrano M, Tschop MH. Sirt1 protects against high-fat diet-induced metabolic damage. Proc Natl Acad Sci U S A 2008;105:9793–8.
13. Purushotham A, Schug TT, Xu Q, Surapureddi S, Guo X, Li X. Hepatocyte-specific deletion of SIRT1 alters fatty acid metabolism and results in hepatic steatosis and inflammation. Cell Metab 2009;9: 327–38.
14. Herranz D, Munoz-Martin M, Canamero M, Mulero F, Martinez-Pastor B, Fernandez-Capetillo O, et al. Sirt1 improves healthy ageing and protects from metabolic syndrome-associated cancer. Nat Commun 2010;1:3.
15. Clinton SK. Lycopene: chemistry, biology, and implications for human health and disease. Nutr Rev 1998;56:35–51.
16. Giovannucci E. Tomatoes, tomato-based products, lycopene, and cancer: review of the epidemiologic literature. J Natl Cancer Inst 1999;91:317–31.
17. Wang XD. Lycopene metabolism and its biological significance. Am J Clin Nutr 2012;96:1214S–22S.
18. Levy J, Walfisch S, Atzmon A, Hirsch K, Khanin M, Linnewiel K, et al. The role of tomato lycopene in cancer prevention. In: Vegetables, whole grains, and their derivatives in cancer prevention. Dordrecht/Heidelberg/London/New York: Springer; 2011. pp. 47–66.
19. Huang CS, Liao JW, Hu ML. Lycopene inhibits experimental metastasis of human hepatoma SK-Hep-1 cells in athymic nude mice. J Nutr 2008;138:538–43.
20. Erhardt A, Stahl W, Sies H, Lirussi F, Donner A, Haussinger D. Plasma levels of vitamin E and carotenoids are decreased in patients with nonalcoholic steatohepatitis (NASH). Eur J Med Res 2011;16:76–8.
21. Astorg P, Gradelet S, Berges R, Suschetet M. Dietary lycopene decreases the initiation of liver preneoplastic foci by diethylnitrosamine in the rat. Nutr Cancer 1997;29:60–8.
22. Wang Y, Ausman LM, Greenberg AS, Russell RM, Wang XD. Dietary lycopene and tomato extract supplementations inhibit nonalcoholic steatohepatitis-promoted hepatocarcinogenesis in rats. Int J Cancer 2010;126:1788–96.
23. Hu KQ, Liu C, Ernst H, Krinsky NI, Russell RM, Wang XD. The biochemical characterization of ferret carotene-9′,10′-monooxygenase catalyzing cleavage of carotenoids in vitro and in vivo. J Biol Chem 2006;281:19327–38.
24. Kiefer C, Hessel S, Lampert JM, Vogt K, Lederer MO, Breithaupt DE, et al. Identification and characterization of a mammalian enzyme catalyzing the asymmetric oxidative cleavage of provitamin A. J Biol Chem 2001;276:14110–6.
25. Lian F, Smith DE, Ernst H, Russell RM, Wang XD. Apo-10′-lycopenoic acid inhibits lung cancer cell growth in vitro, and suppresses lung tumorigenesis in the A/J mouse model in vivo. Carcinogenesis 2007;28:1567–74.
26. Yang CM, Hu TY, Hu ML. Antimetastatic effects and mechanisms of apo-8′-lycopenal, an enzymatic metabolite of lycopene, against human hepatocarcinoma SK-Hep-1 cells. Nutr Cancer 2012;64: 274–85.
27. Chung J, Koo K, Lian F, Hu KQ, Ernst H, Wang XD. Apo-10′-lycopenoic acid, a lycopene metabolite, increases sirtuin 1 mRNA and protein levels and decreases hepatic fat accumulation in ob/ob mice. J Nutr 2012;142:405–10.
28. Gouranton E, Aydemir G, Reynaud E, Marcotorchino J, Malezet C, Caris-Veyrat C, et al. Apo-10′-lycopenoic acid impacts adipose tissue biology via the retinoic acid receptors. Biochim Biophys Acta 2011;1811:1105–14.
29. Lindqvist A, He YG, Andersson S. Cell type-specific expression of beta-carotene 9′,10′-monooxygenase in human tissues. J Histochem Cytochem 2005;53:1403–12.
30. Amengual J, Lobo GP, Golczak M, Li HNM, Klimova T, Hoppel CL, et al. A mitochondrial enzyme degrades carotenoids and protects against oxidative stress. FASEB J 2011;25:948–59.
31. Ford NA, Clinton SK, von Lintig J, Wyss A, Erdman JW Jr. Loss of carotene-9′,10′-monooxygenase expression increases serum and tissue lycopene concentrations in lycopene-fed mice. J Nutr 2010;140: 2134–8.
32. Lietz G, Oxley A, Boesch-Saadatmandi C, Kobayashi D. Importance of beta-carotene 15,15′-monooxygenase 1 (BCMO1) and beta-carotene 9′,10′-dioxygenase 2 (BCDO2) in nutrition and health. Mol Nutr Food Res 2012;56:241–50.
33. Ford NA, Elsen AC, Zuniga K, Lindshield BL, Erdman JW Jr. Lycopene and apo-12′-lycopenal reduce cell proliferation and alter cell cycle progression in human prostate cancer cells. Nutr Cancer 2011;63: 256–63.
34. Vesselinovitch SD, Mihailovich N, Rao KV. Morphology and metastatic nature of induced hepatic nodular lesions in C57BL x C3H F1 mice. Cancer Res 1978;38:2003–10.
35. Kyriazis AP, Koka M, Vesselinovitch SD. Metastatic rate of liver tumors induced by diethylnitrosamine in mice. Cancer Res 1974; 34:2881–6.
36. Katyal S, Oliver JH III, Peterson MS, Ferris JV, Carr BS, Baron RL. Extrahepatic metastases of hepatocellular carcinoma. Radiology 2000;216:698–703.
37. Natsuizaka M, Omura T, Akaike T, Kuwata Y, Yamazaki K, Sato T, et al. Clinical features of hepatocellular carcinoma with extrahepatic metastases. J Gastroenterol Hepatol 2005;20:1781–7.
38. Huang C-S, Chuang C-H, Hu M-L. Effects of lycopene supplementation on plasma and tissue lycopene levels in various rodent strains. Int J Vitam Nutr Res 2006;76:377–84.
39. Sharma V, McNeill JH. To scale or not to scale: the principles of dose extrapolation. Br J Pharmacol 2009;157:907–21.
40. Kopec RE, Riedl KM, Harrison EH, Curley RW Jr, Hruszkewycz DP, Clinton SK, et al. Identification and quantification of apo-lycopenals in fruits, vegetables, and human plasma. J Agric Food Chem 2010;58: 3290–6.
41. Matteoni CA, Younossi ZM, Gramlich T, Boparai N, Liu YC, McCullough AJ. Nonalcoholic fatty liver disease: a spectrum of clinical and pathological severity. Gastroenterology 1999;116:1413–9.
42. Brunt EM, Janney CG, Di Bisceglie AM, Neuschwander-Tetri BA, Bacon BR. Nonalcoholic steatohepatitis: a proposal for grading and staging the histological lesions. Am J Gastroenterol 1999;94: 2467–74.
43. Tanaka T, Suh KS, Lo AM, De Luca LM. p21WAF1/CIP1 is a common transcriptional target of retinoid receptors pleiotropic regulatory mechanism through retinoic acid receptor (RAR)/retinoid X receptor (RXR) heterodimer and RXR/RXR homodimer. J Biol Chem 2007;282: 29987–97.
44. The Jackson Laboratory. C57BL/6J diet-induced obesity (DIO) phenotype. 2013. Available from: http://jaxmice.jax.org/diomice/diomice-phenotypes.html
45. Rodriguez EB, Rodriguez-Amaya DB. Lycopene epoxides and apo-lycopenals formed by chemical reactions and autoxidation

in model systems and processed foods. J Food Sci 2009;74: C674–82.
46. Schmitz HH, Poor CL, Wellman R, Erdman JW Jr. Concentrations of selected carotenoids and vitamin A in human liver, kidney and lung tissue. J Nutr 1991;121:1613.
47. Lian F, Wang XD. Enzymatic metabolites of lycopene induce Nrf2-mediated expression of phase II detoxifying/antioxidant enzymes in human bronchial epithelial cells. Int J Cancer 2008; 123:1262–8.
48. Lian F, Hu KQ, Russell RM, Wang XD. β-Cryptoxanthin suppresses the growth of immortalized human bronchial epithelial cells and non-small-cell lung cancer cells and up-regulates retinoic acid receptor β expression. Int J Cancer 2006;119:2084–9.
49. Liu C, Lian F, Smith DE, Russell RM, Wang XD. Lycopene supplementation inhibits lung squamous metaplasia and induces apoptosis via up-regulating insulin-like growth factor-binding protein 3 in cigarette smoke-exposed ferrets. Cancer Res 2003;63:3138–44.
50. Yeung F, Hoberg JE, Ramsey CS, Keller MD, Jones DR, Frye RA, et al. Modulation of NF-kappaB-dependent transcription and cell survival by the SIRT1 deacetylase. EMBO J 2004;23:2369–80.
51. Chalkiadaki A, Guarente L. High-fat diet triggers inflammation-induced cleavage of SIRT1 in adipose tissue to promote metabolic dysfunction. Cell Metab 2012;16:180–8.
52. Henao-Mejia J, Elinav E, Jin C, Hao L, Mehal WZ, Strowig T, et al. Inflammasome-mediated dysbiosis regulates progression of NAFLD and obesity. Nature 2012;482:179–85.
53. Dixon LJ, Flask CA, Papouchado BG, Feldstein AE, Nagy LE. Caspase-1 as a central regulator of high fat diet-induced non-alcoholic steatohepatitis. PLoS One 2013;8:e56100.
54. Nakanishi K, Sakamoto M, Yamasaki S, Todo S, Hirohashi S. Akt phosphorylation is a risk factor for early disease recurrence and poor prognosis in hepatocellular carcinoma. Cancer 2005;103:307–12.
55. Alexia C, Bras M, Fallot G, Vadrot N, Daniel F, Lasfer M, et al. Pleiotropic effects of PI-3′ kinase/Akt signaling in human hepatoma cell proliferation and drug-induced apoptosis. Ann N Y Acad Sci 2006;1090:1–17.
56. Cuconati A, Mills C, Goddard C, Zhang X, Yu W, Guo H, et al. Suppression of AKT anti-apoptotic signaling by a novel drug candidate results in growth arrest and apoptosis of hepatocellular carcinoma cells. PLoS One 2013;8:e54595.
57. Okada H, Honda M, Campbell JS, Sakai Y, Yamashita T, Takebuchi Y, et al. Acyclic retinoid targets platelet-derived growth factor signaling in the prevention of hepatic fibrosis and hepatocellular carcinoma development. Cancer Res 2012;72:4459–71.
58. Cohen JC, Horton JD, Hobbs HH. Human fatty liver disease: old questions and new insights. Science 2011;332:1519–23.
59. Guturu P, Duchini A. Etiopathogenesis of nonalcoholic steatohepatitis: role of obesity, insulin resistance and mechanisms of hepatotoxicity. Int J Hepatol 2012;2012:212865.
60. Kyriazis AP, Vesselinovitch SD. Transplantability and biological behavior of mouse liver tumors induced by ethylnitrosourea. Cancer Res 1973;33:332–8.